


Parrondo's effect in continuous-time quantum walks

J. J. Ximenes ^{1,*} M. A. Pires,^{2,†} and J. M. Villas-Bôas^{1,‡}

¹*Instituto de Física, Universidade Federal de Uberlândia, 38400-902 Uberlândia, Minas Gerais, Brazil*

²*Universidade Federal de Alagoas, 57480-000, Delmiro Gouveia, Alagoas, Brazil*



(Received 8 November 2023; accepted 23 February 2024; published 19 March 2024)

We present a manifestation of a Parrondo's effect in a continuous-time quantum walk (CTQW). In our protocol we consider a CTQW in the presence of a time-dependent transition defect. Our results show that the alternation between defects, that individually are detrimental to the wavepacket spreading, can paradoxically enhance overall wavepacket propagation. Our findings pave the way for the exploration of unconventional mechanisms that can potentially harness the adverse effects of defects to enhance quantum transport.

DOI: [10.1103/PhysRevA.109.032417](https://doi.org/10.1103/PhysRevA.109.032417)

I. INTRODUCTION

The standard quantum walk (QW) was originally introduced in 1993 [1] in a discrete-time formulation. Subsequently, in 1998, the continuous-time variant of this model was developed [2]. The QW is a lattice-based model exhibiting several interesting properties [3] when compared with the classical random walk (CRW). Comparative analysis between the QW with the classical random walk (CRW) reveals compelling distinctions. First, the spreading of the QW is quadratically faster than the CRW. Second, the QW exhibits a non-Gaussian bimodal probability distribution, in stark contrast to the Gaussian distribution observed in the CRW between both models. The contrast between QWs and CRWs is further accentuated when both models spread on graphs [4]. Recently, the authors of Ref. [5] presented a new difference between the CRW and the QW: the introduction of short-range aperiodic jumps amplifies the spreading of CRWs, while, counterintuitively, it induced an inhibition of wavepacket spreading of QWs.

The wide versatility of QWs leads this model to serve as a computational platform for investigating a broad diversity of phenomena. For instance, with QWs it is possible to explore topological phases [6,7], soliton-like propagation [8], rogue waves [9], trojan's effects [10], the Ramsauer effect [11], q -Gaussian distributions [12], Anderson localization [13,14], hyperballistic regimes [15], and multiple transitions between diffusive, superdiffusive, ballistic, and hyperballistic behavior [16–18]. QWs may also lead to intriguing phenomena [19] and nonmonotonic effects with decoherence [20]. The substantial interest in QWs also stems from their numerous algorithmic applications [21–25] and diverse experimental implementations [26]. The extensive range of possibilities offered by QWs underscores the significance of investigating novel protocols for such model.

In this work, we undertake a theoretical examination of a QW on an infinite line with alternating defects. The subsequent sections of this article are structured as follows. In Sec. II we review articles that are related to our work. In Sec. III we introduce our quantum protocol. In Sec. IV we disclose our results and we discuss our findings considering several measures. In Sec. V we highlight the main differences between our work and the literature and in Sec. VI we present final considerations and further perspectives on our work.

II. RELATED WORKS

We now direct our focus toward more specific works directly relevant to our investigation. The first subsection is devoted to an in-depth exploration of continuous-time quantum walks (CTQWs) and discrete-time quantum walks (DTQWs) with defects. In the second subsection, we review works that demonstrate the manifestation of the Parrondo's effect (PE) within the context of DTQWs, as there is no realization of such phenomenon in CTQWs, so far.

A. QWs with defects

The exploration of defects in QWs has evolved systematically, offering valuable insights into how they shape the wavepacket dynamics. The work of Childs *et al.* [4] offered early insights into how a single defect can disrupt wavepacket propagation of CTQWs on graphs, laying the groundwork for further investigations. Zhang *et al.* [27] observed the localization effect in one-dimensional (1D)-CTQWs with single-point phase defects, contributing to the understanding of defect-induced phenomena. Keating *et al.* [28] explored CTQWs with Cauchy-distributed defects, shedding light on the localization effects associated with specific defect distributions. Agliari *et al.* [29] investigated CTQWs with traps placed in fractal structures, revealing the behavior of wavepackets in nontrivial environments. Izaac *et al.* [30] conducted a study on 1D-CTQWs in the presence of multiple defects. Their results showed the presence of resonance behavior. Benedetti *et al.* [31] addressed the utilization of CTQWs as quantum probes

*jeffersonximenes@ufu.br

†marcelo.pires@delmiro.ufal.br

‡boas@ufu.br

for characterizing defects and perturbations within network structures. Li *et al.* [32] conducted a comprehensive study on CTQWs with potential defects, as well as DTQWs with phase defects, considering single and double position defects on a one-dimensional lattice. Later, Li and Wang [33] analytically investigated a model that is equivalent to a scattering transmission of 1D-CTQW with defects. More recently, Teles and Amorim [34] studied how defects in DTQWs affect the return probability of a quantum particle. Kiumi and Saito [35] provided analytical results for two-phase DTQWs with one defect. All these studies have enriched our comprehension of defect-induced effects in various QW models.

B. Parrondo's effect in QWs

The PE is traditionally formulated in terms of a combination of losing games that can produce a winning game [36,37]. Over the years such a phenomenon has been observed in such a wide variety of fields [38–40] that today the PE can be defined more generally as the emergence of favorable outcomes from combinations of unfavorable scenarios.

The earliest attempts to establish Parrondian QWs can be traced to Refs. [41–43]. These works were successful in the short-time, however they fail to obtain a stable PE in the long-time. Similar efforts to introduce a Parrondo's paradox within QWs did not succeed in the asymptotic limit [44,45]. Nowadays, there are several protocols for obtaining the Parrondo's effect or Parrondo-like effects in DTQWs [46–62] or related models [40,63–65]. Notably, in Refs. [59–61] the authors showed scenarios in which the PE in QWs were associated with an enhancement in the corresponding coin-space entanglement between the internal (spin) and external (position) degrees of freedom. In Ref. [62] the first experimental verification of a quantum Parrondo walk within a quantum optics setup was presented.

III. MODEL

In this section, we describe step by step our quantum protocol.

A. CTQW

The Hamiltonian governing the dynamics of a CTQW for a single quantum particle, quantum walker, moving only between nearest neighbor sites within a uniform one-dimensional lattice can be expressed as

$$H_0 = \epsilon \sum_j |j\rangle\langle j| - \gamma \sum_j (|j+1\rangle\langle j| + |j-1\rangle\langle j|), \quad (1)$$

where ϵ represents the constant potential energy, while γ denotes the transition rate. This last term will be a constant fixed during simulations, whereas other constants will be given as a function of it; so that, without loss of generality, the behavior remains unchanged for any chosen value in the given relations. Thus, given an initial state $|\Psi(t=0)\rangle$, the evolution of the system can be described by the equation

$$i \frac{\partial}{\partial t} |\Psi(t)\rangle = H_0 |\Psi(t)\rangle, \quad (2)$$

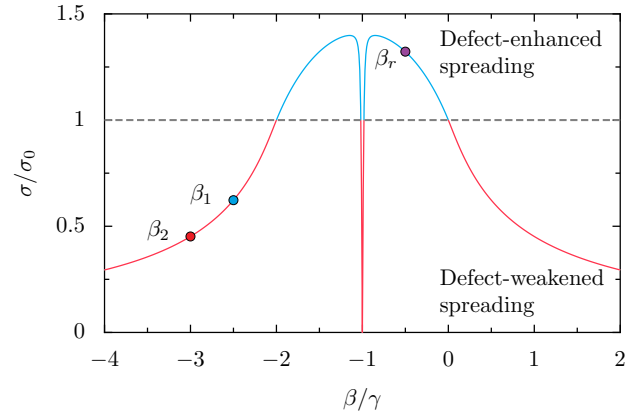


FIG. 1. Relative standard deviation σ/σ_0 as a function of β for $\gamma t = 2000$. We use the reference σ_0 for the defect-free case. The dashed line separates the zone in which defects enhances spreading (above) from the region in which defects reduces spreading (below). The $\beta_1 = -2.5\gamma$ and $\beta_2 = -3\gamma$ are the values used in simulations.

in which we set $\hbar = 1$. The evolution of the system is assessed through the calculation of the probability distribution

$$P_j(t) = |\langle j | \psi(t) \rangle|^2. \quad (3)$$

To quantify the rate of spreading during this propagation, we analyze the standard deviation

$$\sigma = \sqrt{\overline{j^2} - \overline{j}^2}, \quad (4)$$

where the expectation value of the power of j , j^n , is given by $\overline{j^n} = \sum_j j^n P_j$.

B. Transition defects

The incorporation of transition defects within the lattice structure can be achieved by altering the transition rates between lattice sites. Following the approach of Li and Wang [66], in the context of a particle residing at site $j = d$ with nearest neighbors, the introduction of a transition defect is accomplished by the inclusion of the term

$$H_d = -(|d\rangle\langle d+1| + |d+1\rangle\langle d| + |d-1\rangle\langle d| + |d\rangle\langle d-1|). \quad (5)$$

This term is characterized by an associated transition rate denoted as β . The resultant modification of the Hamiltonian can be expressed as

$$H_0 + \beta H_d. \quad (6)$$

In this study, we consider $\epsilon = 0$ and $d = 0$. Li and Wang [66] observed that for a specific value of $\beta = -0.5\gamma$, the evolution of $\sigma(t)$ surpasses that of the defect-free scenario. We first extend their results and we show in Fig. 1 that there is a non-monotonic transition from the regime with defect-weakened spreading to the regime with defect-enhanced spreading. When $\beta = -\gamma$, the particle remains confined in site $j = d$ because the transition rate becomes null $\beta + \gamma = 0$ in Eq. (6) for neighbors of this point; therefore, the propagation in the remaining sites is canceled. So that, from this point, symmetry is observed.

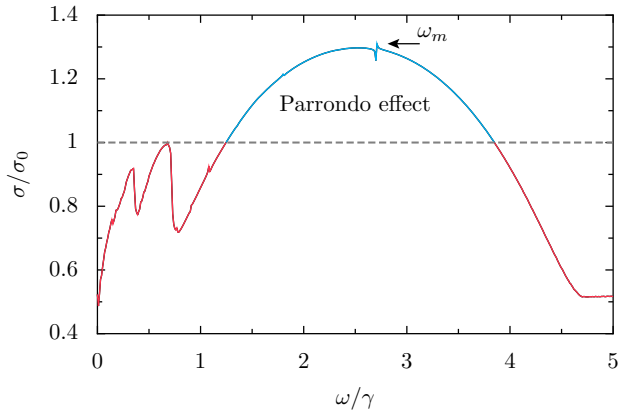


FIG. 2. Relative standard deviation σ/σ_0 as a function of w for $\gamma t = 2000$. The dashed line separates the zone in which defects enhances spreading (above) from the region in which defects reduces spreading (below).

C. Protocol for alternation

Following the conventional mechanism of Parrondo's game, we implement an alternation between two scenarios with unfavorable outcomes, that in our model are characterized by weak spreading. To achieve this goal, a time-periodic function with a period of T , denoted as $f(t+T) = f(t)$, is defined such that, for $0 \leq t \leq T$,

$$f(t) = \begin{cases} \beta_2, & \text{if } t \leq \frac{T}{2}, \\ \beta_1, & \text{if } t > \frac{T}{2}, \end{cases} \quad (7)$$

where the corresponding frequency is $w = 2\pi/T$. By selecting two distinct transition rates, denoted as β_1 and β_2 , the Hamiltonian governing this mechanism can be defined as

$$H = H_0 + f(t)H_d. \quad (8)$$

Consequently, the Hamiltonian takes on the form of Eq. (6) during intervals of time $T/2$. Within each of these intervals, the transition rate different, allowing for a switching between two distinct modes.

IV. RESULTS AND DISCUSSION

In this section, we present the results and discussion of our Parrondian QW. Our analysis involves a comprehensive comparison with the QW in which defects typically have a detrimental effect on wavepacket spreading (associated with β_1 and β_2 as illustrated in Fig. 1). Additionally, we compare our results with the standard defect-free QW.

Following the model given by the Eq. (8), we alternate the dynamics with $\beta_1 = -2.5\gamma$ and $\beta_2 = -3\gamma$ for a range of frequencies depicted in Fig. 2. The measures σ and σ_0 quantify the wavepacket spreading for scenarios with and without defects, respectively. The dynamics characterized by β_1 and β_2 are selected, both exhibiting $\sigma/\sigma_0 < 1$ (reduced spreading). The results show the emergence of an interesting zone in which the Parrondo's paradox is detected. Specifically, it is possible to observe that the switching between two regimes with $\sigma/\sigma_0 < 1$ (weakened spreading) can lead to the appearance of a regime with $\sigma/\sigma_0 > 1$ (enhanced spreading).

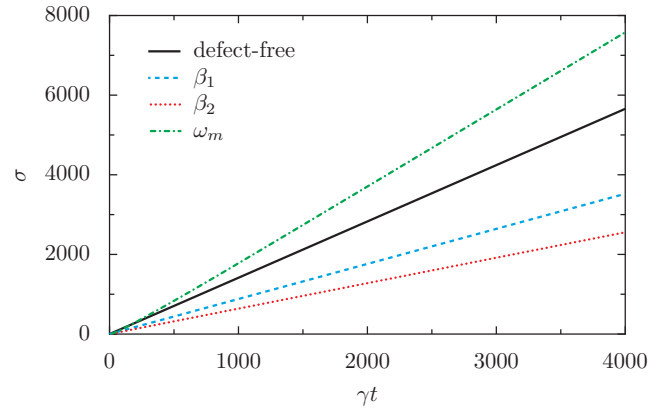


FIG. 3. Time evolution of the relative standard deviation σ/σ_0 for our Parrondian QW (with $\omega_m = 2.71\gamma$), the defect-free QW, as well as the QW with defects. The fastest spreading occurs for the Parrondian QW.

In Fig. 3, we observe that the time evolution for the standard deviation of the Parrondo case (with frequency w_m as illustrated in Fig. 2) surpasses that of the model with weak spreading induced by defects (for β_1 and β_2). Notably, the Parrondian QW also overcomes the standard deviation for the setting without defects. Thus, our protocol provides a QW with alternating defects that can be tuned to exhibit an enhanced spreading rate compared to the usual QW model. We also checked that our model is still ballistic. That is, in contrast to previous investigations [15–18], our accelerated QW model does not present a hyperballistic scaling.

To gain insights into the spatial distribution of wavepackets across the N sites at a given instant of time, we calculate two distributional measures. First, we compute the Shannon entropy given by

$$S = - \sum_j P_j \log_{10} P_j. \quad (9)$$

Additionally, we evaluate the inverse participation ratio (IPR) given by

$$\text{IPR} = \left(\sum_j P_j^2 \right)^{-1}. \quad (10)$$

Both S and IPR have two well-defined extremes. For a wavepacket entirely distributed across the N sites: $S = \log_{10} N$ and $\text{IPR} = N$. On the other hand, for a wavepacket fully localized $S = 0$ and $\text{IPR} = 1$.

The results for the Shannon entropy are shown in Fig. 4. We see that our Parrondian QW (line associated with ω_m) has a wavepacket more distributed across the lattice than the cases with weak spreading (lines associated with β_1 and β_2). However, we observe that the defect-free QW produces more Shannon entropy than our Parrondian QW, indicating that it is more delocalized than our model. This behavior is further confirmed with the results of the IPR, as presented in Fig. 5. The weak spreading (for β_1 and β_2) is nearly localized, in contrast to the defect-free QW, which is significantly distributed across the lattice. Between both cases we observe our Parrondian QW with an intermediate IPR. These results show that both

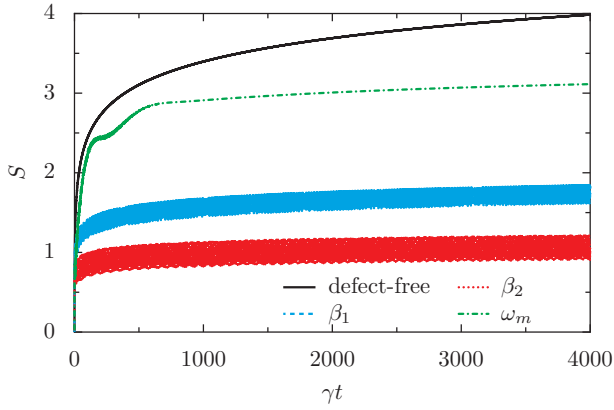


FIG. 4. Time evolution of the Shannon entropy S for the same models and parameters presented in the Fig. 3. The defect-free QW exhibits the highest values for Shannon entropy.

S and IPR are in agreement and highlight that the Parrondian QW is accompanied by a wavepacket distributed over fewer sites across the lattice when compared to the defect-free QW.

To gain deeper insights into the underlying mechanisms of our Parrondian QW, we conducted a comprehensive analysis of its associated probability distribution. In Figs. 6(a) and 6(c) it is evident that the central region of the defect-free QW distribution has a higher probability of being populated than the corresponding region of the Parrondian QW distribution. Such result is in agreement with the insights obtained from the Shannon entropy and IPR.

The wavepacket spreading is evaluated by the standard deviation, which is a global measure (assessed for the entire lattice). Thus, let us analyze a local version of this measure. To grasp local contributions for the spreading we compute the relative quadratic deviation (RQD) [67]

$$\text{RQD}(j) = (j - \bar{j})^2 P_j. \quad (11)$$

It is evident from Figs. 6(b) and 6(d) that the local contributions to the global standard deviation are primarily determined by the peaks at the edges of the probability distribution. Comparing the maximum RQD of Parrondo case RQD_{mp} with

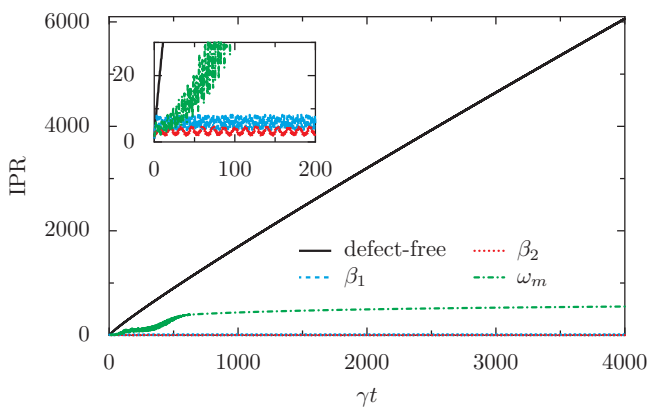


FIG. 5. Time evolution of the IPR for the same models and parameters presented in the Fig. 3. The IPR of the defect-free QW presents the highest values.

defect-free case RQD_{md} , we obtain $\text{RQD}_{mp}/\text{RQD}_{md} \approx 4.44$, which is in accordance with the respective ratio of maximum probabilities $P_{mp}/P_{md} \approx 4.47$.

In summary, all the aforementioned insights collectively indicate that the enhancement of the spreading observed in the Parrondian QW stems from a reduction in probability within the central region, resulting in a relative accumulation at the border of the QW distribution.

V. COMPARISON WITH PREVIOUS PARRONDIAN PHENOMENA IN QWS

In this section, we highlight three crucial points regarding our work in comparison to prior literature addressing the Parrondo effect in QWs [46–62].

First, even though defects have already been introduced in DTQWs (as shown in Sec. II.A), there is no work that has used defects to produce a Parrondian QW.

Second, all the aforementioned works focused on the DTQW, which is a model that has a versatile coin operator. In contrast, the CTQW lacks a quantum coin, making the generation of a Parrondo effect a challenging task. Thus, our protocol is not merely an extension of those employed for generating Parrondian phenomena in DTQWs.

Third, the usual form of Parrondo's paradox found in QWs is characterized by the combination of two unfavorable outcomes [or losing games, $P_i(x)$ skewed towards $x < 0$] that gives rise to a favorable outcome [or winning game, $P_i(x)$ skewed towards $x > 0$]. In contrast, we adopt an alternative perspective where we do not focus on payoff-based analyses or measures related to the asymmetries in the probability flux or current. Instead, our emphasis lies on the inherent transport phenomenon, where we demonstrate that our Parrondian CTQW enhances the wavepacket spreading (as shown in Fig. 3).

VI. FINAL REMARKS

We conducted an investigation into the transport properties of CTQWs in the presence of time-dependent transition defects. Our model was formulated to account for alternating configurations in which these defects traditionally play a role in reducing the wavepacket dispersion.

Our results reveal the manifestation of a Parrondian effect in the domain of CTQWs. In our protocol, we show that the alternating use of two unfavorable setups, where defects decelerate wavepacket spreading, can lead to scenarios in which the wavepacket spreads faster than the defect-free CTQW.

Our findings offer a fresh perspective on how to use defects, which are usually seen as detrimental, to improve quantum transport. This approach has the potential to enhance the efficiency and reliability of quantum transport systems, making our results promising for future developments in the field of quantum transport. As comprehensively exemplified in Sec. I, QWs are connected to a plethora of phenomena in several domains of research, thus our results can provide insights about the role of alternating defects in applied fields [21–25] as well as fundamental areas [6,7].

In future works, we plan to investigate the influence of temporal switching, incorporating both positive and negative

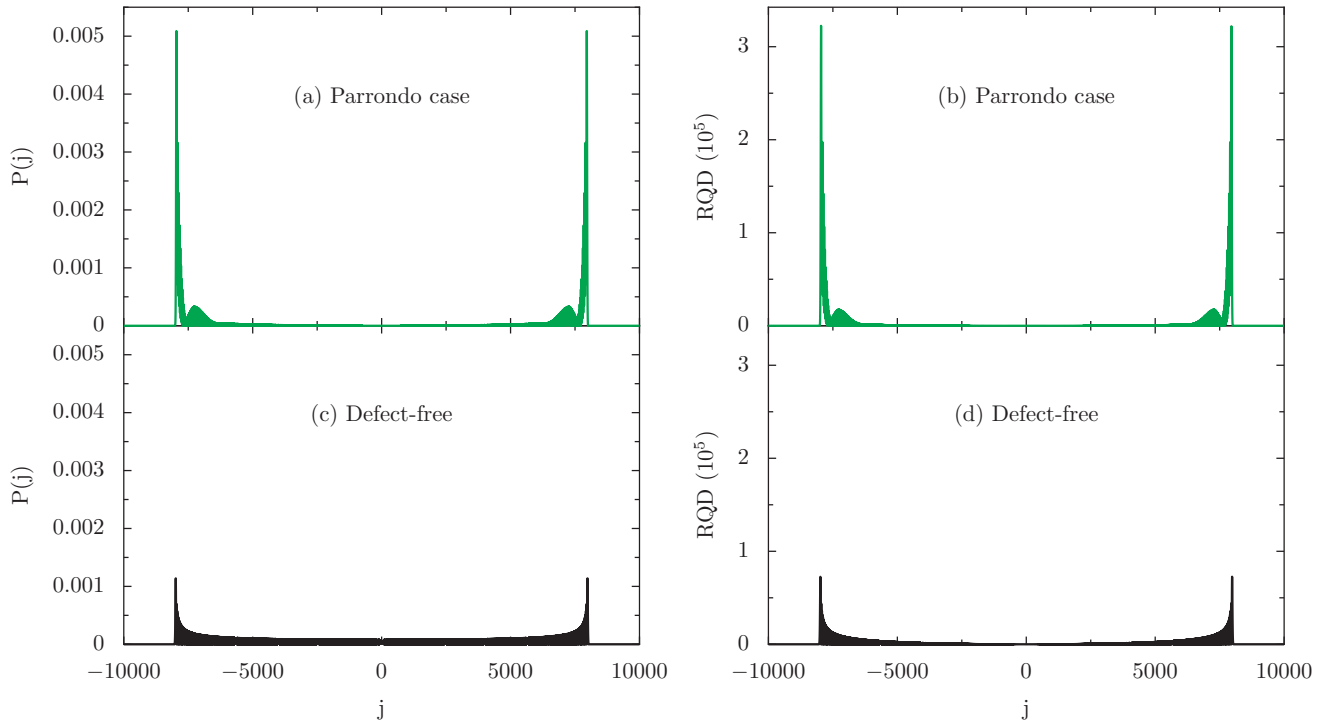


FIG. 6. Comparison of probability distribution and relative quadratic deviation between case defect-free QW and Parrondian QW for $\gamma t = 4000$.

correlations, on the manifestation of the PE in CTQWs. As shown recently [67] negative correlated temporal disorder is able to produce nontrivial effects in QWs. The investigation of the effects of chaotic switching [68,69] in our protocol is also an important research endeavor. We will also modify the model to enhance the propagation with these alternations, as

well as analyze this dynamic in networks beyond the one-dimensional case.

ACKNOWLEDGMENT

We acknowledge the FAPEMIG for financial support.

-
- [1] Y. Aharonov, L. Davidovich, and N. Zagury, Quantum random walks, *Phys. Rev. A* **48**, 1687 (1993).
 - [2] E. Farhi and S. Gutmann, Quantum computation and decision trees, *Phys. Rev. A* **58**, 915 (1998).
 - [3] J. Kempe, Quantum random walks: An introductory overview, *Contemp. Phys.* **44**, 307 (2003).
 - [4] A. M. Childs, E. Farhi, and S. Gutmann, An example of the difference between quantum and classical random walks, *Quantum Info. Proc.* **1**, 35 (2002).
 - [5] M. A. Pires and S. M. D. Queirós, Quantum walks with sequential aperiodic jumps, *Phys. Rev. E* **102**, 012104 (2020).
 - [6] T. Kitagawa, M. S. Rudner, E. Berg, and E. Demler, Exploring topological phases with quantum walks, *Phys. Rev. A* **82**, 033429 (2010).
 - [7] J. Wu, W.-W. Zhang, and B. C. Sanders, Topological quantum walks: Theory and experiments, *Front. Phys.* **14**, 61301 (2019).
 - [8] J. P. Mendonça, F. A. B. F. de Moura, M. L. Lyra, and G. M. A. Almeida, Emergent nonlinear phenomena in discrete-time quantum walks, *Phys. Rev. A* **101**, 062335 (2020).
 - [9] A. R. C. Buarque, W. S. Dias, F. A. B. F. de Moura, M. L. Lyra, and G. M. A. Almeida, Rogue waves in discrete-time quantum walks, *Phys. Rev. A* **106**, 012414 (2022).
 - [10] H. S. Ghizoni and E. P. M. Amorim, Trojan quantum walks, *Braz. J. Phys.* **49**, 168 (2019).
 - [11] H. T. Lam and K. Y. Szeto, Ramsauer effect in a one-dimensional quantum walk with multiple defects, *Phys. Rev. A* **92**, 012323 (2015).
 - [12] Y. Shikano, T. Wada, and J. Horikawa, Discrete-time quantum walk with feed-forward quantum coin, *Sci. Rep.* **4**, 4427 (2014).
 - [13] S. Derevyanko, Anderson localization of a one-dimensional quantum walker, *Sci. Rep.* **8**, 1795 (2018).
 - [14] J. Ghosh, Simulating Anderson localization via a quantum walk on a one-dimensional lattice of superconducting qubits, *Phys. Rev. A* **89**, 022309 (2014).
 - [15] G. Di Molfetta, D. O. Soares-Pinto, and S. M. D. Queirós, Elephant quantum walk, *Phys. Rev. A* **97**, 062112 (2018).
 - [16] M. A. Pires, G. Di Molfetta, and S. M. D. Queirós, Multiple transitions between normal and hyperballistic diffusion in quantum walks with time-dependent jumps, *Sci. Rep.* **9**, 19292 (2019).
 - [17] C. B. Naves, M. A. Pires, D. O. Soares-Pinto, and S. M. D. Queirós, Enhancing entanglement with the generalized elephant quantum walk from localized and delocalized states, *Phys. Rev. A* **106**, 042408 (2022).

- [18] C. B. Naves, M. A. Pires, D. O. Soares-Pinto, and S. M. D. Queirós, Quantum walks in two dimensions: controlling directional spreading with entangling coins and tunable disordered step operator, *J. Phys. A: Math. Gen.* **56**, 125301 (2023).
- [19] V. Kendon and B. Tregenna, Decoherence can be useful in quantum walks, *Phys. Rev. A* **67**, 042315 (2003).
- [20] A. C. Oliveira, R. Portugal, and R. Donangelo, Decoherence in two-dimensional quantum walks, *Phys. Rev. A* **74**, 012312 (2006).
- [21] A. Ambainis, Quantum walks and their algorithmic applications, *Int. J. Quantum. Inform.* **01**, 507 (2003).
- [22] R. Portugal, *Quantum Walks and Search Algorithms* (Springer, New York, 2013).
- [23] S. E. Venegas-Andraca, Quantum walks for computer scientists, *Synth. Lect. Quantum Comput.* **1**, 1 (2008).
- [24] S. E. Venegas-Andraca, Quantum walks: a comprehensive review, *Quantum Info. Proc.* **11**, 1015 (2012).
- [25] K. Kadian, S. Garhwal, and A. Kumar, Quantum walk and its application domains: A systematic review, *Computer Science Review* **41**, 100419 (2021).
- [26] J. Wang and K. Manouchehri, *Physical Implementation of Quantum Walks* (Springer, New York, 2013).
- [27] R. Zhang, P. Xue, and J. Twamley, One-dimensional quantum walks with single-point phase defects, *Phys. Rev. A* **89**, 042317 (2014).
- [28] J. P. Keating, N. Linden, J. C. F. Matthews, and A. Winter, Localization and its consequences for quantum walk algorithms and quantum communication, *Phys. Rev. A* **76**, 012315 (2007).
- [29] E. Agliari, A. Blumen, and O. Mülken, Quantum-walk approach to searching on fractal structures, *Phys. Rev. A* **82**, 012305 (2010).
- [30] J. A. Izaac, J. B. Wang, and Z. J. Li, Continuous-time quantum walks with defects and disorder, *Phys. Rev. A* **88**, 042334 (2013).
- [31] C. Benedetti, M. A. C. Rossi, and M. G. A. Paris, Continuous-time quantum walks on dynamical percolation graphs, *Europhys. Lett.* **124**, 60001 (2019).
- [32] Z. J. Li, J. A. Izaac, and J. B. Wang, Position-defect-induced reflection, trapping, transmission, and resonance in quantum walks, *Phys. Rev. A* **87**, 012314 (2013).
- [33] Z.-J. Li and J. Wang, An analytical study of quantum walk through glued-tree graphs, *J. Phys. A: Math. Gen.* **48**, 355301 (2015).
- [34] L. I. da S. Teles and E. P. M. Amorim, Localization in quantum walks with a single lattice defect: A comparative study, *Braz. J. Phys.* **51**, 911 (2021).
- [35] C. Kiumi and K. Saito, Eigenvalues of two-phase quantum walks with one defect in one dimension, *Quantum Info. Proc.* **20**, 171 (2021).
- [36] J. M. R. Parrondo, How to cheat a bad mathematician, in EEC HCM Network on Complexity and Chaos (ERBCHRX-CT940546), ISI, Torino, Italy (1996).
- [37] G. P. Harmer and D. Abbott, Losing strategies can win by Parrondo's paradox, *Nature (London)* **402**, 864 (1999).
- [38] D. Abbott, Asymmetry and disorder: A decade of Parrondo's paradox, *Fluct. Noise Lett.* **09**, 129 (2010).
- [39] K. H. Cheong, J. M. Koh, and M. C. Jones, Paradoxical survival: examining the Parrondo effect across biology, *BioEssays* **41**, 1900027 (2019).
- [40] J. W. Lai and K. H. Cheong, Parrondo's paradox from classical to quantum: A review, *Nonlinear Dyn.* **100**, 849 (2020).
- [41] D. A. Meyer and H. Blumer, Parrondo games as lattice gas automata, *J. Stat. Phys.* **107**, 225 (2002).
- [42] D. A. Meyer and H. Blumer, Quantum Parrondo games: biased and unbiased, *Fluct. Noise Lett.* **02**, L257 (2002).
- [43] D. A. Meyer, Noisy quantum parrondo games, in *Fluctuations and Noise in Photonics and Quantum Optics*, Vol. 5111 (International Society for Optics and Photonics, Bellingham, WA, 2003), pp. 344–350.
- [44] A. P. Flitney, Quantum Parrondo's games using quantum walks, [arXiv:1209.2252](https://arxiv.org/abs/1209.2252).
- [45] M. Li, Y.-S. Zhang, and G.-C. Guo, Quantum Parrondo's games constructed by quantum random walks, *Fluct. Noise Lett.* **12**, 1350024 (2013).
- [46] A. P. Flitney, D. Abbott, and N. F. Johnson, Quantum walks with history dependence, *J. Phys. A: Math. Gen.* **37**, 7581 (2004).
- [47] J. Košík, J. A. Miszczyk, and V. Bužek, Quantum Parrondo's game with random strategies, *J. Mod. Opt.* **54**, 2275 (2007).
- [48] C. M. Chandrashekar and S. Banerjee, Parrondo's game using a discrete-time quantum walk, *Phys. Lett. A* **375**, 1553 (2011).
- [49] J. Rajendran and C. Benjamin, Playing a true parrondo's game with a three-state coin on a quantum walk, *Europhys. Lett.* **122**, 40004 (2018).
- [50] J. Rajendran and C. Benjamin, Implementing Parrondo's paradox with two-coin quantum walks, *R. Soc. Open Sci.* **5**, 171599 (2018).
- [51] T. Machida and F. A. Grünbaum, Some limit laws for quantum walks with applications to a version of the Parrondo paradox, *Quantum Info. Proc.* **17**, 241 (2018).
- [52] Z. Walczak and J. H. Bauer, Noise-induced Parrondo's paradox in discrete-time quantum walks, *Phys. Rev. E* **108**, 044212 (2023).
- [53] Z. Walczak and J. H. Bauer, Parrondo's paradox in quantum walks with three coins, *Phys. Rev. E* **105**, 064211 (2022).
- [54] Z. Walczak and J. H. Bauer, Parrondo's paradox in quantum walks with deterministic aperiodic sequence of coins, *Phys. Rev. E* **104**, 064209 (2021).
- [55] G. Trautmann, C. Groiseau, and S. Wimberger, Parrondo's paradox for discrete-time quantum walks in momentum space, *Fluct. Noise Lett.* **21**, 2250053 (2022).
- [56] J. W. Lai and K. H. Cheong, Parrondo effect in quantum coin-toss simulations, *Phys. Rev. E* **101**, 052212 (2020).
- [57] J. W. Lai, J. R. A. Tan, H. Lu, Z. R. Yap, and K. H. Cheong, Parrondo paradoxical walk using four-sided quantum coins, *Phys. Rev. E* **102**, 012213 (2020).
- [58] A. Mielke, Quantum Parrondo games in low-dimensional hilbert spaces, [arXiv:2306.16845](https://arxiv.org/abs/2306.16845).
- [59] M. A. Pires and S. M. D. Queirós, Parrondo's paradox in quantum walks with time-dependent coin operators, *Phys. Rev. E* **102**, 042124 (2020).
- [60] D. K. Panda, B. V. Govind, and C. Benjamin, Generating highly entangled states via discrete-time quantum walks with Parrondo sequences, *Physica A* **608**, 128256 (2022).
- [61] M. Jan, N. A. Khan, and G. Xianlong, Territories of Parrondo's paradox and its entanglement dynamics in quantum walks, *Eur. Phys. J. Plus* **138**, 65 (2023).
- [62] M. Jan, Q.-Q. Wang, X.-Y. Xu, W.-W. Pan, Z. Chen, Y.-J. Han, C.-F. Li, G.-C. Guo, and D. Abbott, Experimental realization

- of Parrondo's paradox in 1D quantum walks, *Adv. Quantum Technol.* **3**, 1900127 (2020).
- [63] A. P. Flitney, J. Ng, and D. Abbott, Quantum Parrondo's games, *Physica A* **314**, 35 (2002).
- [64] P. Gawron and J. A. Mischak, Quantum implementation of Parrondo's paradox, *Fluct. Noise Lett.* **05**, L471 (2005).
- [65] S. Banerjee, C. M. Chandrashekar, and A. K. Pati, Enhancement of geometric phase by frustration of decoherence: A Parrondo-like effect, *Phys. Rev. A* **87**, 042119 (2013).
- [66] Z.-J. Li and J. Wang, Single-point position and transition defects in continuous time quantum walks, *Sci. Rep.* **5**, 13585 (2015).
- [67] M. A. Pires and S. M. D. Queirós, Negative correlations can play a positive role in disordered quantum walks, *Sci. Rep.* **11**, 4527 (2021).
- [68] J. W. Lai and K. H. Cheong, Chaotic switching for quantum coin Parrondo's games with application to encryption, *Phys. Rev. Res.* **3**, L022019 (2021).
- [69] A. Panda and C. Benjamin, Order from chaos in quantum walks on cyclic graphs, *Phys. Rev. A* **104**, 012204 (2021).